Phototheranostics Using Erythrocyte-Based Particles

Subjects: Materials Science, Biomaterials

Contributor: Bahman Anvari

There has been a recent increase in the development of delivery systems based on red blood cells (RBCs) for light-mediated imaging and therapeutic applications. These constructs are able to take advantage of the immune evasion properties of the RBC, while the addition of an optical cargo allows the particles to be activated by light for a number of promising applications.

delivery systems red blood cells photothermal therapy photodynamic therapy cancer imaging

1. Introduction

In recent decades, numerous types of constructs have been developed for the delivery of therapeutic and imaging payloads to target sites of interest. The overarching goals of engineered delivery systems are to protect the payload from non-specific interactions with biomolecules and other molecular entities in the milieu of physiological environments, and minimize clearance by the immune system so that sufficient amounts of the payload can reach the target site to achieve the desired efficacy without inducing non-specific toxicity and reducing harmful off-target side effects [1].

A contemporary approach in engineering of delivery systems is based on the use of cells or cell-derived constructs to encapsulate the desired payload, or cell membranes to coat the payload. Examples include delivery systems based on macrophages, lymphocytes, neutrophils, and stems cells [2][3]. A fundamental principle underlying the use of cell-based or cell-derived systems is that the built-in mosaic of the cell membrane can provide the camouflaging machinery to protect the payload from recognition by immune cells and increase the bioavailability of the payload.

Red blood cells (RBCs) (erythrocytes) are a particularly promising delivery system due to the presence of membrane proteins including CD47, which prevents phagocytic uptake by macrophages, as well as decay-accelerating factor (DAF) (CD55) and CD59, which protect the RBCs from complement damage and cell lysis by preventing the formation of membrane-attack complexes [4]. The presence of these “self-markers” on RBCs has the potential to increase the circulation of a desired payload embedded within an RBC-based construct as a result of protecting the payload from recognition and subsequent removal or destruction by the immune system. One of the earliest examples of RBCs being used as carriers dates back to 1973, when Ihler et al. demonstrated the successful loading of RBCs with various enzymes [5]. There has been a significant increase in RBC-derived

constructs in recent years, especially in the field of nanomedicine, where RBCs have reportedly been used as carriers for not only enzymes, but antibiotics, nanoparticles (NPs), and various drugs as well [6]. More recently, RBC-based payload delivery systems have been extensively reviewed [4][6][7][8][9][10][11][12], and new sub-fields, such as systems designed for the delivery of cancer therapeutics [13] and vascular imaging [14], are emerging. A particular use of RBC-derived constructs is in relation to loading of optical cargos such as quantum dots (QDs) [15][16][17], metallic materials [18][19][20], and organic molecules [21][22][23], in order to use the constructs for optical imaging and sensing, and phototherapeutic applications. This review specifically covers the development of RBC-derived constructs for light-based theranostics and summarizes some of the current potential clinical applications for these constructs. We provide a listing of the acronyms used in this manuscript in Table 1.

Table 1. List of acronyms.

Acronym	Definition
AFM	Atomic force microscopy
ALP	Alkaline phosphatase
ALT	Alanine aminotransferase
BSA	Bovine serum albumin
CD	Cluster of differentation
Ce6	Chlorin e6
Cy5	Cyanine 5
DACHPt	1,2-diaminocyclohexane-platinum (II)
DAF	Decay-accelerating factor
DAPI	4′,6-diamidino-2-phenylindole
DiR	1, 1-dioctadecyl-3, 3, 3, 3-tetramethylindotricarbocyanine iodide
DOX	Doxorubicin
DSPE	1,2-distearoly-sn-glycero-3-phosphoethanolamine
EDTA	Ethylenediamine tetraacetic acid
EGs	Erythrocyte ghosts
EPR	Enhanced permeability and retention
FA	Folic acid

Acronym	Definition
Fe_3O_4	Iron oxide
FITC	Fluorescein isothiocyanate
HCPT	10-hydroxycamptothecin
H_2O_2	Hydrogen peroxide
ICG	Indocyanine green
ICG-EGs	Erythrocyte ghosts loaded with ICG
ICG-nEGs	Nano-sized erythrocyte ghosts loaded with ICG
IG	Immunoglobulin
IL	Interleukin
IR	Infrared
MB	Methylene Blue
$MgCl_2$	Magnesium choloride
MOF	Metal–organic framework
$MoSe_2$	Molybdenum diselenide
MRI	Magnetic resonance imaging
$NaGdF_4$:Yb, Tm	Ytterbium and thulium doped sodium gadolinium fluoride
$NaYF_4$:Yb/Er	Ytterbium and erbium doped sodium yttrium fluoride
NHS	N-hydroxysuccinimide
nEGs	Nano-sized erythrocyte ghosts
NIR	Near infrared
NPs	Nanoparticles
PBS	Phosphate buffer saline
PDT	Photodynamic therapy
PEG	Polyethylene glycol
PFC	Perfluorocarbon

Acronym	Definition
PS	Phosphatidylserine
PTT	Photothermal therapy
PWS	Port wine stain
QPs	Quantum dots
RB	Rose bengal
RBCs	Red blood cells
RGD	Arginylglycylasparatic acid
ROS	Reactive oxygen species
SDS-PAGE	Sodium dodecyl sulphate–polyacrylamide gel electrophoresis
TEM	Transmission electron microscope
TiO_2	Titanium dioxide
TNF	Tumor necrosis factor-alpha
tPA	Tissue plasminogen activator
TPC	5,10,15,20-tetraphenylchlorin
UCST	Upper critical solution temperature
UV	Ultraviolet
UCNPs	Upconversion nanoparticles
$ZnF_{16}Pc$	Zinc hexadecafluorophthalocyanine

cargo in used for a number of optical cargos such as various metals and semiconductors. For example, Ren et al. coated iron oxide (Fe_3O_4) magnetic nanoclusters with RBC membranes for photothermal therapy (PTT) [24]. Gold NPs, such as gold nanorods fabricated by Li et al., have also been coated with RBC membranes for use in PTT [25]. Semiconducting materials, such as the $MoSe_2$ nanosheets designed by He et al., were similarly coated with RBC membranes, again for PTT [26]. NPs made from organic molecules have also been coated with RBC membranes. For example, Ye et al. coated spherical NPs comprised of chemodrug 10-hydroxycamptothecin (HCPT) and the near-infrared (NIR) dye indocyanine green (ICG) with RBC membranes, and used them for combined chemotherapy and PTT [27]. Chen et al. prepared hollow mesoporous Prussian blue (PB) NPs loaded with the chemotherapeutic drug doxorubicin (DOX), and coated them with RBC membranes for combined PTT and chemotherapy [28].

Another common optical cargo is upconversion nanoparticles (UCNPs). These NPs are usually made from rare-earth elements and are capable of converting longer wavelengths of light, such as NIR wavelengths, into shorter wavelengths, such as visible or UV light [29]. For example, Ding et al. prepared $NaYF_4$:Yb/Er UCNPs coated with RBC membranes and containing the photosensitizer merocyanine 540 (MC540) [30]. Here, the UCNPs excited by

980 nm laser light resulted in luminescence in the 530–550 nm range, which was able to excite the MC540 for photodynamic therapy (PDT).

The examples mentioned thus far have involved coating a NP made from a material capable of interacting with light. However, there are some instances where NPs themselves are loaded with an optical cargo before being coated with an RBC membrane. For example, Yang et al. fabricated triblock copolymer nanoparticles loaded with the dye IR780 for phototherapy and docetaxel (DTX) for chemotherapy [31]. These particles were then coated with RBC membranes for enhanced circulation. In addition, there are some constructs where the RBC membrane is used to coat a non-optical cargo, and the optical cargo is incorporated into the construct using other methods. For example, Su et al. loaded polymeric NPs with paclitaxel for chemotherapy, and then coated the particles with RBC membranes that had the cyanine dye 1, 1-dioctadecyl-3, 3, 3, 3-tetramethylindotricarbocyanine iodide (DiR) inserted into the lipid bilayer for PTT [32]. Here, the optical cargo is not in the core of the construct, but is instead in the membrane coating itself.

All of these examples show that there are a large number of constructs that can be coated with RBC membranes. In order to coat a cargo with the RBC membrane, whole blood is first washed with an isotonic buffer such as phosphate-buffered saline (PBS) to isolate the RBCs. The isolated RBCs are treated with a hypotonic buffer to deplete hemoglobin from the RBCs, resulting in erythrocyte ghosts (EGs). The EGs can then be scaled from the micro- to the nano-sized dimensions. Common methods for size reduction are mechanical extrusion, sonication, or a combination of the two. During mechanical extrusion, EGs are pushed through membranes with pores of a predetermined size, usually on the order of 200–800 nm. This leads to membrane lysis and reformation into smaller vesicles [33]. Sonication, or the application of sound waves with varying frequencies, is another cell disruption method [34]. Sonicating EGs also results in membrane rupture, and the subsequent reformation of nano-sized membranes [35]. A schematic illustrating the steps for formation of nano-sized EGs (nEGs) is shown in Figure 1.

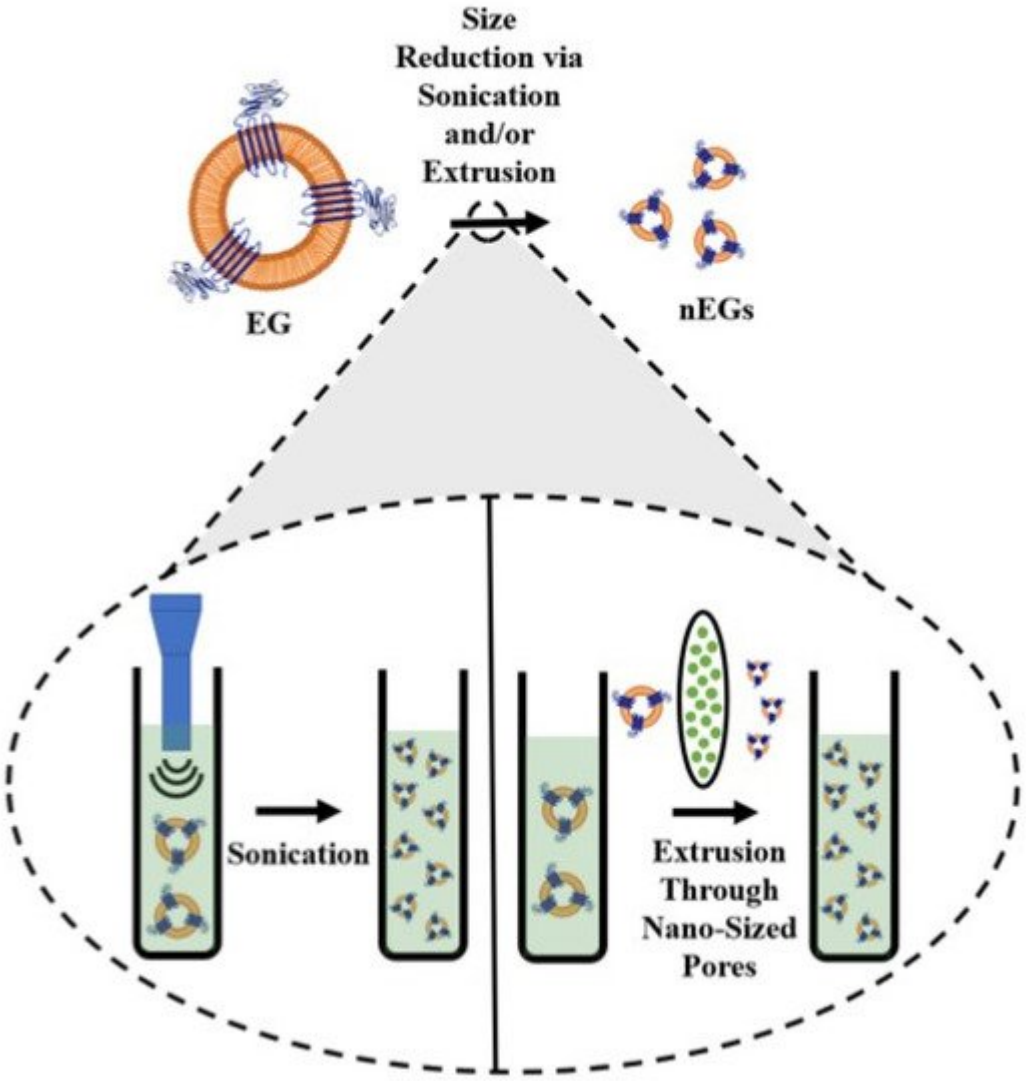

Figure 1. Schematic illustration of RBC membrane coating. RBCs are depleted of their hemoglobin using a hypotonic treatment to form erythrocyte ghosts (EGs). For illustration purposes, CD47 is shown as one of the RBC transmembrane proteins retained on EGs. The inset illustrates the sonication and extrusion size reduction methods. During sonication, sound waves are applied to EGs, while during extrusion, the EGs are pushed through filters with nano-sized pores, both of which result in formation of nEGs.

Since both sonication and extrusion result in membrane rupture, they can be used not only to reduce the change EGs to nEGs, but also to facilitate coating of an optical cargo. Mixing nEGs with a NP and repeating the sonication and/or extrusion facilitates the coating of the cargo with the RBC membrane, resulting in a construct with a core-shell morphology where the NP is coated by a membrane layer. Transmission electron microscope (TEM) images show that the RBC membrane conforms to the shape of the coated substrate. This has been shown in the work done by Rao et al., where coating hexagonal UCNPs with RBC membranes resulted in a hexagonal construct for cancer imaging [36]. Wang et al. have also developed spherical bovine serum albumin (BSA) nanoconstructs that encapsulate ICG and the chemodrug gambogic acid, and when coated in RBC membranes also result in a spherical nanoconstruct for chemotherapy and PTT [37]. These examples show a uniform membrane coating on a NP core. In addition to confirming the membrane coating using imaging, RBC membrane coatings have been

confirmed by SDS-PAGE [36][38][39][40], as well as Western blots demonstrating the presence of CD47 on the final construct [31][41]. Our proteomics analysis based on tandem mass spectrometry confirm that CD47, CD55, CD59 and other membrane and cytoskeletal proteins including α-spectrin are retained in EGs loaded with ICG (ICG-EGs) (Figure 2).

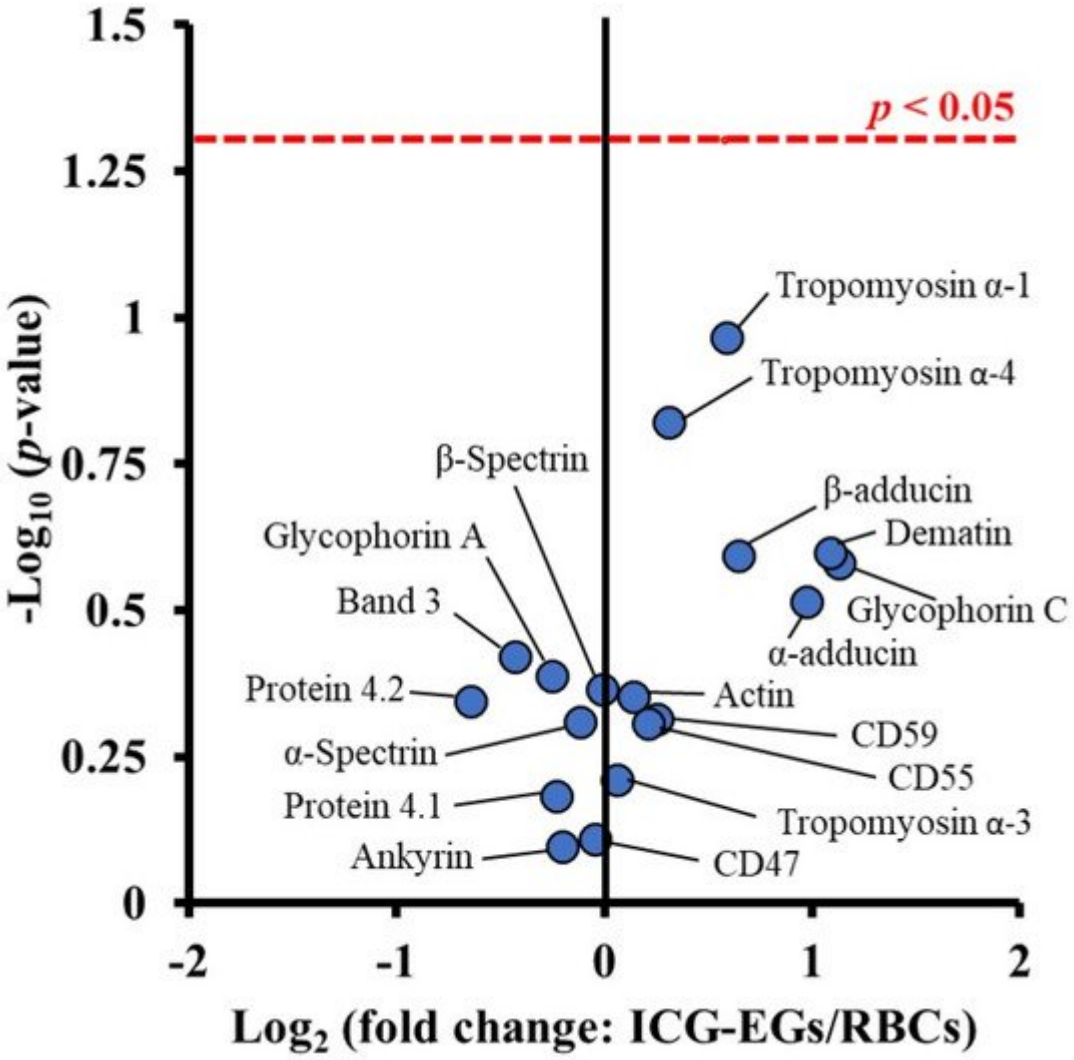

Figure 2. Volcano plot associated with proteomics analysis of human RBCs, and ICG-EGs. Each dot represents a particular protein. There are no statistically significant differences in the ratios of ICG-EGs proteins to RBCs proteins located below the red dashed line.

Constructs that employ RBC membranes as a substrate coating have also been shown to be stable, with many constructs showing minimal changes in size after storage of up to one week [42][43]. We have demonstrated that after 12 h of storage in the dark at 4 and 37 °C, fluorescence emission of nEGs loaded with ICG (ICG-nEGs) was retained, whereas there was nearly a 40% reduction in the emission for free ICG [44]. The zeta-potentials of ICG-EGs and ICG-nEGs formed by extrusion were ~ −12.8 mV, and not significantly different from that for RBCs [44], indicating that the carboxyl groups of sialoglycoproteins, which are associated with much of the negative charge of RBCs, were retained during the fabrication of the particles. We have also found that there is only approximately a

5% reduction in ICG monomer absorbance of ICG after 8 days of storage in isotonic PBS at 4 °C in the dark [45]. We have determined that only approximately 5% of ICG leaks from ICG-nEGs over 48 h of storage at 37 °C [46]. We have also investigated the optical and physical properties of ICG-nEGs stored at −20 °C for up to 8 weeks and then thawed at room temperature [47]. Our results showed that the hydrodynamic diameter, zeta-potential, absorbance, and NIR fluorescence emission of ICG-nEGs were retained following the freeze–thaw cycle. The ability of ICG-nEGs in NIR fluorescence imaging of ovarian cancer cells, as well as their biodistribution in reticuloendothelial organs of healthy Swiss Webster mice after the freeze–thaw cycle were similar to those for freshly prepared ICG-nEGs.

While most of the previous examples have involved constructs where the RBC membranes coat a single NP, there are exceptions. For instance, Liu et al. encapsulated ICG in anionic BSA nanoclusters to form complexes with the chemotherapeutic 1,2-diaminocyclohexane-platinum (II) (DACHPt) [48]. These nanoclusters were coated with RBC membranes, resulting in constructs with an outer membrane shell and containing multiple BSA-based nanoclusters inside. In addition, researchers have shown that RBC membrane coatings are not limited to NPs. Gao et al. designed microparticles comprised of RBC-shaped magnetic hemoglobin containing Fe_3O_4 NPs and ICG, as magnetically-navigating PDT mediators [49].

2.2. Constructs That Use the RBC As a Carrier

While most light-based RBC-derived constructs use the RBC membrane as a substrate coating, there are a growing number of constructs that use the RBC as a carrier. Constructs that use the RBC as a carrier can have a variety of optical cargos, including organic molecules [50][51][52] and NPs made from various metals [18] or semiconductors [53][54]. While constructs that use the RBC membrane as a coating primarily use sonication and/or extrusion to facilitate substrate coating, there are a number of different loading methods for constructs that use the RBC as a carrier. Loading methods can be applied directly to RBCs, as well as EGs and nEGs. However, the vast majority of RBC-derived carriers are fabricated from RBCs. These methods can be broadly divided into those that load a cargo to the interior of the carrier, and those that load the cargo to the exterior of the construct.

2.2.1. Methods for Interior Loading of an Optical Cargo

Hypotonic Loading

The most common loading methods for RBC carrier constructs are those that involve hypotonic buffers. When RBCs are placed in a hypotonic buffer they swell, causing the formation of pores for removal of intracellular components, but also allowing the internal loading of the cargo [50]. For example, Wu et al., using a hypotonic treatment, were able to simultaneously load RBCs with DOX, magnetic NPs, and QDs capable of fluorescence emission [15]. We have used a similar method to load EGs with ICG using Sorenson's buffer, resulting in micron-sized light-responsive constructs [46]. Our group has also applied this method to nEGs, where we first extruded EGs to form nEGs before incubating them with Sorenson's buffer and ICG, resulting in the loading of ICG into the nEGs [46]. Therefore, hypotonic loading methods can be applied to RBCs, EGs, and nEGs. RBCs can also be loaded using hypotonic dialysis. Here, the RBCs are typically mixed with a cargo in a dialysis bag, which is then

exposed to a hypotonic buffer, again leading to the formation of pores through which the cargo can enter the RBCs [55]. Figure 3 shows a schematic illustrating optical cargo loading of RBCs, EGs, and nEGs.

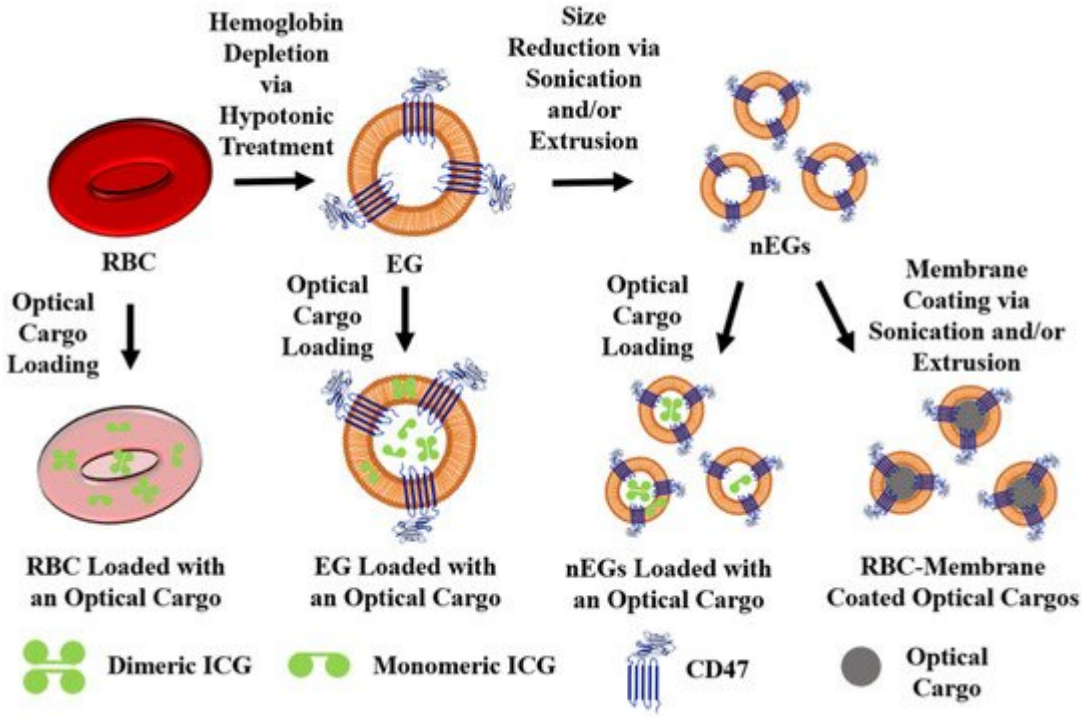

Figure 3. Schematic illustration of RBCs, EGs, and nEGs loaded with an optical cargo to serve as RBC-derived carriers. For illustration purposes CD47 is shown as one of the RBC transmembrane proteins retained on EGs. A representative spherical nanoparticle, to be coated with RBC membrane, is shown as the optical cargo for constructs formed using sonication and/or extrusion. Indocyanine green (ICG) is shown in its dimeric and monomeric forms as a representative optical cargo.

It is interesting to note that in some cases, loading the RBCs with an optical cargo in a hypotonic buffer has been reported to preserve the biconcave disk shape and size of native RBCs. For example, Jiang et al. were able to load mouse RBCs with fluorescent silicon NPs hypotonically, resulting in constructs with the biconcave disk morphology ~6 μm in diameter [53]. Here, the hypotonic buffer was 0.5× PBS containing 2 mM ATP and 3 mM glutathione, and the mixture was incubated for 45 min at 4 °C. Jiang et al. showed that after the RBCs were resealed, the silicon NPs were visible inside the RBCs [53]. However, hypotonically loading the optical cargo does not always preserve the biconcave morphology of native RBCs, as can be seen by the constructs fabricated by Bustamante López and Meissner [56]. After using a hypotonic lysis buffer to load bovine erythrocytes with fluorescein isothiocyanate (FITC) glycylglycine conjugates, the resulting constructs were significantly smaller and had less hemoglobin compared to native erythrocytes. When analyzed using atomic force microscopy (AFM), the authors also found that the loaded constructs were more rounded and had a rougher surface compared to native erythrocytes. Here, the lysis buffer contained $MgCl_2$, EDTA, phosphate buffer, and urea [56].

As demonstrated by the two previous examples, the buffer choice for hypotonic loading can vary, which may be why hypotonic loading does not always produce constructs that preserve native RBC morphology. A number of

different buffers have been used for hypotonic dialysis [55], but there are no clear trends for hypotonic buffer choice when it comes to loading optical cargos. Another factor potentially affecting the morphology of the construct is the species source of blood. For instance, Jiang et al. used mouse blood for their constructs [53], while Bustamante López and Meissner used bovine blood [56]. Many constructs are fabricated using mouse blood. This includes the constructs engineered by Marvin et al., with RBC morphology preserved after using dialysis to load RBCs in a hypotonic PBS buffer with 6 mM glucose [57]. It is possible that differences between the RBCs, such as membrane composition, age, and size, could have an effect on how the cells react to hypotonic loading methods. It is important to note that for clinical translation, the constructs will ultimately need to be fabricated using human RBCs. It is known that there are a number of structural differences between mouse and human RBCs, such as size and membrane protein composition [58]. Further research is needed to determine whether hypotonic loading methods used on human RBCs will still preserve the native RBC morphology. More research is also needed on the effects of using different hypotonic buffers for the loading procedure, as well as the effect of the type of optical cargo being loaded.

Another important factor to consider with hypotonic treatment is the potential for phosphatidylserine (PS) exposure. PS is generally confined to the inner leaflet of erythrocytes [59], and its exposure leads to macrophage recognition and subsequent clearance of erythrocytes from circulation [60]. Wang et al. have shown that EGs prepared by incubating mouse RBCs in 5 mM NaH_2PO_3/Na_2HPO_3 for 5 min at 4 °C have significantly more PS exposure compared to native mouse RBCs [61]. Sun et al. showed similar PS exposure results for murine RBC-derived EGs, but showed that RBCs loaded with DOX via hypotonic dialysis did not show elevated PS exposure levels [62]. We have also shown elevated expression levels of PS on μEGs and nEGs following hypotonic treatment of bovine RBCs [63]. Therefore, the effect of hypotonic loading on PS exposure needs to be more thoroughly understood, particularly for carriers derived from human RBCs.

Other Methods for Interior Optical Cargo Loading

Electroporation is another method for cargo loading that involves the application of an electric field to the membranes, which results in the formation of pores through which materials can cross the membrane [64]. Bustamante Lopéz and Meissner were able to use electroporation to load bovine RBC membranes with glycylglycine-conjugated FITC [56]. Compared to loading using a hypotonic buffer, however, RBCs loaded via electroporation had a significantly lower loading efficiency [56].

Another loading method involves extrusion to load small organic molecules. In this case, the RBC membrane does not coat the cargo and is instead used as a nano-sized carrier. For example, we mixed EGs derived from bovine RBCs with ICG-BSA and extruded the solution, resulting in nano-sized constructs capable of being used for cancer cell imaging applications [65]. It is important to note that using extrusion to load organic molecules will result in a nano-sized construct. While these two examples demonstrate that there are potentially RBC interior loading methods that do not use a hypotonic buffer, hypotonic loading mechanisms are more common for loading optical cargos. More research is needed to determine whether these alternative loading methods offer a significant advantage over hypotonic loading methods. In addition, both of these examples were conducted with bovine RBCs.

Mouse and human RBCs may respond differently to these loading techniques, indicating another area for further research.

Optical Cargo Embedding in the Lipid Bilayer

Some organic molecules are capable of directly interacting with RBC membranes, allowing them to be embedded into the lipid membrane of the RBC. For example, chlorin e6 (Ce6) is a lipophilic molecule capable of interacting with lipid membranes [66]. Gao et al. and Sun et al. have demonstrated that Ce6 can be embedded in RBC membranes by mixing [52][67]. Sun et al. used the Ce6-embedded RBC membrane as a coating for PB NPs [67], suggesting that embedding optical cargos can be combined with using RBC membranes as a substrate coating. Gao et al. demonstrated that they were able to combine the hypotonic dialysis loading of DOX into RBCs with Ce6 embedding in the RBC lipid bilayer [52]. In addition, Gao et al. were able to show that while DOX was loaded to the interior of the RBCs, Ce6 was localized to the membrane of the RBCs. Not only do these two studies demonstrate that optical cargos have the potential to be loaded into RBCs through simple mixing, but they also demonstrate that multiple loading methods can be used to fabricate a single construct. Another lipophilic dye, DiR, has been used for cell membrane labeling [68], and is another potential optical cargo that can be directly embedded in RBC membranes. Su et al. have demonstrated that DiR is capable of being embedded into the lipid membranes of nEGs, which are then used to coat paclitaxel-load polymeric NPs [32]. While this example of an optical cargo being embedded in the lipid bilayer was also ultimately used for substrate coating, it also suggests that lipophilic dyes can be embedded into the lipid membranes of EGs and nEGs. However, organic molecules are the only optical cargos that have been embedded into the lipid bilayer of RBC-derived constructs, so this loading method may have limited applications for other optical cargos, such as metallic NPs.

2.2.2. Methods for Exterior Loading of an Optical Cargo

While RBC-derived constructs employed as carriers usually involve loading an optical cargo to the interior, or in some cases into the lipid membrane bilayer of the construct, there are some examples of the optical cargo being incorporated onto the surface. For example, some optical cargos are able to adsorb directly to the surface of RBCs. Delcea et al. were able to incorporate gold NPs into their constructs using adsorption. They suggest that the adsorption is possible due to interactions between the positively charged NPs and the negatively charged glycocalyx on the RBC membrane [18].

It has also been suggested that organic molecules are capable of adsorbing to RBCs; however, the results have not been as promising. Sun et al. report that they were able to adsorb ICG to the surface of RBCs, but that the ICG was easily washed away in serum-supplemented media [62]. Flower and Kling similarly showed that while ICG is capable of adsorbing to RBCs, the amount of ICG that could be loaded was almost half the amount that could be loaded into RBCs hypotonically [69]. While there is potential for optical cargos to adsorb directly to RBCs, more research needs to be done to determine the types of optical cargos it is appropriate for, as well as determining how the adsorption is accomplished for those appropriate optical cargos.

Another method for attaching an optical cargo to the surface of RBC-derived constructs is functionalization. Here, a lipid linker is used to attach the optical cargo to the surface of the construct. A common lipid linker is 1,2-distearoly-sn-glycero-3-phosphoethanolamine-N-[χ(polyethylene glycol)] (DSPE-PEG-χ) where χ can be a number of functional groups. DSPE is able to insert itself into the lipid bilayer of the RBC membranes, similar to the lipid-insertion methods outlined by Fang et al. [70], resulting in the desired molecule being attached to the surface of the RBC membrane. Wang et al. incubated RBCs with DSPE-PEG-biotin, which enabled them to attach various avidin-functionalized UCNPs to the RBCs [71][72]. This method takes advantage of the strong and highly specific interaction between biotin and avidin [73], resulting in constructs that preserve the biconcave morphology of native RBCs [71][72]. Other groups have used other lipid linkers to biotinylate RBCs. For example, Tang et al. used biotin-X-NHS, which was able to attach to neutravidin, and in turn able to bind to their biotinylated ferritin nano-capsules loaded with the optical cargo $ZnF_{16}Pc$ [74]. Wang et al. used sulfo-NHS-LC-biotin to biotinylate RBCs, which could then bind to Ce6-coated iron oxide NPs that were conjugated to avidin [61].

References

1. Pattni, B.S.; Torchilin, V.P. Targeted Drug Delivery Systems: Strategies and Challenges. In Targeted Drug Delivery : Concepts and Design; Devarajan, P.V., Jain, S., Eds.; Advances in Delivery Science and Technology; Springer International Publishing: Cham, Switzerland, 2015; pp. 3–38. ISBN 978-3-319-11355-5.
2. Yoo, J.-W.; Irvine, D.J.; Discher, D.E.; Mitragotri, S. Bio-Inspired, Bioengineered and Biomimetic Drug Delivery Carriers. Nat. Rev. Drug Discov. 2011, 10, 521–535.
3. Sier, V.Q.; de Vries, M.R.; van der Vorst, J.R.; Vahrmeijer, A.L.; van Kooten, C.; Cruz, L.J.; de Geus-Oei, L.-F.; Ferreira, V.; Sier, C.F.M.; Alves, F.; et al. Cell-Based Tracers as Trojan Horses for Image-Guided Surgery. Int. J. Mol. Sci. 2021, 22, 755.
4. Han, X.; Wang, C.; Liu, Z. Red Blood Cells as Smart Delivery Systems. Bioconjug. Chem. 2018, 29, 852–860.
5. Ihler, G.M.; Glew, R.H.; Schnure, F.W. Enzyme Loading of Erythrocytes. Proc. Natl. Acad. Sci. USA 1973, 70, 2663–2666.
6. Koleva, L.; Bovt, E.; Ataullakhanov, F.; Sinauridze, E. Erythrocytes as Carriers: From Drug Delivery to Biosensors. Pharmaceutics 2020, 12, 276.
7. Muzykantov, V.R. Drug Delivery by Red Blood Cells: Vascular Carriers Designed by Mother Nature. Expert Opin. Drug Deliv. 2010, 7, 403–427.
8. Hu, C.-M.J.; Fang, R.H.; Zhang, L. Erythrocyte-Inspired Delivery Systems. Adv. Healthc. Mater. 2012, 1, 537–547.
9. Zarrin, A.; Foroozesh, M.; Hamidi, M. Carrier Erythrocytes: Recent Advances, Present Status, Current Trends and Future Horizons. Expert Opin. Drug Deliv. 2014, 11, 433–447.

10. Villa, C.H.; Seghatchian, J.; Muzykantov, V. Drug Delivery by Erythrocytes: “Primum Non Nocere”. Transfus. Apher. Sci. Off. J. World Apher. Assoc. Off. J. Eur. Soc. Haemapheresis 2016, 55, 275–280.
11. Villa, C.H.; Anselmo, A.C.; Mitragotri, S.; Muzykantov, V. Red Blood Cells: Supercarriers for Drugs, Biologicals, and Nanoparticles and Inspiration for Advanced Delivery Systems. Adv. Drug Deliv. Rev. 2016, 106, 88–103.
12. Villa, C.H.; Cines, D.B.; Siegel, D.L.; Muzykantov, V. Erythrocytes as Carriers for Drug Delivery in Blood Transfusion and Beyond. Transfus. Med. Rev. 2017, 31, 26–35.
13. Sun, D.; Chen, J.; Wang, Y.; Ji, H.; Peng, R.; Jin, L.; Wu, W. Advances in Refunctionalization of Erythrocyte-Based Nanomedicine for Enhancing Cancer-Targeted Drug Delivery. Theranostics 2019, 9, 6885–6900.
14. Antonelli, A.; Sfara, C.; Magnani, M. Intravascular Contrast Agents in Diagnostic Applications: Use of Red Blood Cells to Improve the Lifespan and Efficacy of Blood Pool Contrast Agents. Nano Res. 2017, 10, 731–766.
15. Wu, Z.; de Ávila, B.E.-F.; Martín, A.; Christianson, C.; Gao, W.; Kun Thamphiwatana, S.; Escarpa, A.; He, Q.; Zhang, L.; Wang, J. RBC Micromotors Carrying Multiple Cargos towards Potential Theranostic Applications. Nanoscale 2015, 7, 13680–13686.
16. Guo, X.; Zhang, Y.; Liu, J.; Yang, X.; Huang, J.; Li, L.; Wan, L.; Wang, K. Red Blood Cell Membrane-Mediated Fusion of Hydrophobic Quantum Dots with Living Cell Membranes for Cell Imaging. J. Mater. Chem. B 2016, 4, 4191–4197.
17. Li, C.; Yang, X.-Q.; An, J.; Cheng, K.; Hou, X.-L.; Zhang, X.-S.; Hu, Y.-G.; Liu, B.; Zhao, Y.-D. Red Blood Cell Membrane-Enveloped O2 Self-Supplementing Biomimetic Nanoparticles for Tumor Imaging-Guided Enhanced Sonodynamic Therapy. Theranostics 2020, 10, 867–879.
18. Delcea, M.; Sternberg, N.; Yashchenok, A.M.; Georgieva, R.; Bäumler, H.; Möhwald, H.; Skirtach, A.G. Nanoplasmonics for Dual-Molecule Release through Nanopores in the Membrane of Red Blood Cells. ACS Nano 2012, 6, 4169–4180.
19. Wang, D.; Dong, H.; Li, M.; Cao, Y.; Yang, F.; Zhang, K.; Wenhao, D.; Wang, C.; Zhang, X. Erythrocyte–Cancer Hybrid Membrane Camouflaged Hollow Copper Sulfide Nanoparticles for Prolonged Circulation Life and Homotypic-Targeting Photothermal/Chemotherapy of Melanoma. ACS Nano 2018, 12, 5241–5252.
20. Liu, Z.; Wang, J.; Qiu, K.; Liao, X.; Rees, T.W.; Ji, L.; Chao, H. Fabrication of Red Blood Cell Membrane-Camouflaged Cu2−xSe Nanoparticles for Phototherapy in the Second near-Infrared Window. Chem. Commun. 2019, 55, 6523–6526.
21. Milanick, M.A.; Ritter, S.; Meissner, K. Engineering Erythrocytes to Be Erythrosensors: First Steps. Blood Cells. Mol. Dis. 2011, 47, 100–106.

22. Bahmani, B.; Bacon, D.; Anvari, B. Erythrocyte-Derived Photo-Theranostic Agents: Hybrid Nano-Vesicles Containing Indocyanine Green for near Infrared Imaging and Therapeutic Applications. Sci. Rep. 2013, 3.
23. Wang, L.; Chen, S.; Pei, W.; Huang, B.; Niu, C. Magnetically Targeted Erythrocyte Membrane Coated Nanosystem for Synergistic Photothermal/Chemotherapy of Cancer. J. Mater. Chem. B 2020.
24. Ren, X.; Zheng, R.; Fang, X.; Wang, X.; Zhang, X.; Yang, W.; Sha, X. Red Blood Cell Membrane Camouflaged Magnetic Nanoclusters for Imaging-Guided Photothermal Therapy. Biomaterials 2016, 92, 13–24.
25. Li, J.; Yao, H.; Wei, Z.; Li, X.; Mu, X.; Wu, L.; Liu, Y.; Jiang, J. Seedless Synthesis of Gold Nanorods with (+)-Catechin-Assisted and Red Blood Cell Membranes Coating as a Biomimetic Photothermal Agents. Mater. Technol. 2018, 33, 825–834.
26. He, L.; Nie, T.; Xia, X.; Liu, T.; Huang, Y.; Wang, X.; Chen, T. Designing Bioinspired 2D MoSe2 Nanosheet for Efficient Photothermal-Triggered Cancer Immunotherapy with Reprogramming Tumor-Associated Macrophages. Adv. Funct. Mater. 2019, 29.
27. Ye, S.; Wang, F.; Fan, Z.; Zhu, Q.; Tian, H.; Zhang, Y.; Jiang, B.; Hou, Z.; Li, Y.; Su, G. Light/PH-Triggered Biomimetic Red Blood Cell Membranes Camouflaged Small Molecular Drug Assemblies for Imaging-Guided Combinational Chemo-Photothermal Therapy. ACS Appl. Mater. Interfaces 2019, 11, 15262–15275.
28. Chen, W.; Zeng, K.; Liu, H.; Ouyang, J.; Wang, L.; Liu, Y.; Wang, H.; Deng, L.; Liu, Y.-N. Cell Membrane Camouflaged Hollow Prussian Blue Nanoparticles for Synergistic Photothermal-/Chemotherapy of Cancer. Adv. Funct. Mater. 2017, 27, 1605795.
29. Wang, M.; Abbineni, G.; Clevenger, A.; Mao, C.; Xu, S. Upconversion Nanoparticles: Synthesis, Surface Modification and Biological Applications. Nanomed. Nanotechnol. Biol. Med. 2011, 7, 710–729.
30. Ding, H.; Lv, Y.; Ni, D.; Wang, J.; Tian, Z.; Wei, W.; Ma, G. Erythrocyte Membrane-Coated NIR-Triggered Biomimetic Nanovectors with Programmed Delivery for Photodynamic Therapy of Cancer. Nanoscale 2015, 7, 9806–9815.
31. Yang, Q.; Xiao, Y.; Yin, Y.; Li, G.; Peng, J. Erythrocyte Membrane-Camouflaged IR780 and DTX Coloading Polymeric Nanoparticles for Imaging-Guided Cancer Photo–Chemo Combination Therapy. Mol. Pharm. 2019, 16, 3208–3220.
32. Su, J.; Sun, H.; Meng, Q.; Yin, Q.; Zhang, P.; Zhang, Z.; Yu, H.; Li, Y. Bioinspired Nanoparticles with NIR-Controlled Drug Release for Synergetic Chemophotothermal Therapy of Metastatic Breast Cancer. Adv. Funct. Mater. 2016, 26, 7495–7506.

33. Guo, P.; Huang, J.; Zhao, Y.; Martin, C.R.; Zare, R.N.; Moses, M.A. Nanomaterial Preparation by Extrusion through Nanoporous Membranes. Small 2018, 14, 1703493.
34. Borthwick, K.A.J.; Coakley, W.T.; McDonnell, M.B.; Nowotny, H.; Benes, E.; Gröschl, M. Development of a Novel Compact Sonicator for Cell Disruption. J. Microbiol. Methods 2005, 60, 207–216.
35. Kuo, Y.-C.; Wu, H.-C.; Hoang, D.; Bentley, W.E.; D'Souza, W.D.; Raghavan, S.R. Colloidal Properties of Nanoerythrosomes Derived from Bovine Red Blood Cells. Langmuir 2016, 32, 171–179.
36. Rao, L.; Meng, Q.-F.; Bu, L.-L.; Cai, B.; Huang, Q.; Sun, Z.-J.; Zhang, W.-F.; Li, A.; Guo, S.-S.; Liu, W.; et al. Erythrocyte Membrane-Coated Upconversion Nanoparticles with Minimal Protein Adsorption for Enhanced Tumor Imaging. ACS Appl. Mater. Interfaces 2017, 9, 2159–2168.
37. Wang, P.; Jiang, F.; Chen, B.; Tang, H.; Zeng, X.; Cai, D.; Zhu, M.; Long, R.; Yang, D.; Kankala, R.K.; et al. Bioinspired Red Blood Cell Membrane-Encapsulated Biomimetic Nanoconstructs for Synergistic and Efficacious Chemo-Photothermal Therapy. Colloids Surf. B Biointerfaces 2020, 189, 110842.
38. Zhu, D.-M.; Xie, W.; Xiao, Y.-S.; Suo, M.; Zan, M.-H.; Liao, Q.-Q.; Hu, X.-J.; Chen, L.-B.; Chen, B.; Wu, W.-T.; et al. Erythrocyte Membrane-Coated Gold Nanocages for Targeted Photothermal and Chemical Cancer Therapy. Nanotechnology 2018, 29, 084002.
39. Rao, L.; Meng, Q.-F.; Huang, Q.; Liu, P.; Bu, L.-L.; Kondamareddy, K.K.; Guo, S.-S.; Liu, W.; Zhao, X.-Z. Photocatalytic Degradation of Cell Membrane Coatings for Controlled Drug Release. Adv. Healthc. Mater. 2016, 5, 1420–1427.
40. Wang, S.; Yin, Y.; Song, W.; Zhang, Q.; Yang, Z.; Dong, Z.; Xu, Y.; Cai, S.; Wang, K.; Yang, W.; et al. Red-Blood-Cell-Membrane-Enveloped Magnetic Nanoclusters as a Biomimetic Theranostic Nanoplatform for Bimodal Imaging-Guided Cancer Photothermal Therapy. J. Mater. Chem. B 2020, 8, 803–812.
41. Peng, J.; Yang, Q.; Li, W.; Tan, L.; Xiao, Y.; Chen, L.; Hao, Y.; Qian, Z. Erythrocyte-Membrane-Coated Prussian Blue/Manganese Dioxide Nanoparticles as H2O2-Responsive Oxygen Generators To Enhance Cancer Chemotherapy/Photothermal Therapy. ACS Appl. Mater. Interfaces 2017, 9, 44410–44422.
42. Li, M.; Fang, H.; Liu, Q.; Gai, Y.; Yuan, L.; Wang, S.; Li, H.; Hou, Y.; Gao, M.; Lan, X. Red Blood Cell Membrane-Coated Upconversion Nanoparticles for Pretargeted Multimodality Imaging of Triple-Negative Breast Cancer. Biomater. Sci. 2020, 8, 1802–1814.
43. Jiang, Q.; Luo, Z.; Men, Y.; Yang, P.; Peng, H.; Guo, R.; Tian, Y.; Pang, Z.; Yang, W. Red Blood Cell Membrane-Camouflaged Melanin Nanoparticles for Enhanced Photothermal Therapy. Biomaterials 2017, 143, 29–45.

44. Tang, J.C.; Partono, A.; Anvari, B. Near-Infrared-Fluorescent Erythrocyte-Mimicking Particles: Physical and Optical Characteristics. IEEE Trans. Biomed. Eng. 2019, 66, 1034–1044.
45. Mac, J.T.; Nuñez, V.; Burns, J.M.; Guerrero, Y.A.; Vullev, V.I.; Anvari, B. Erythrocyte-Derived Nano-Probes Functionalized with Antibodies for Targeted near Infrared Fluorescence Imaging of Cancer Cells. Biomed. Opt. Express 2016, 7, 1311–1322.
46. Vankayala, R.; Mac, J.T.; Burns, J.M.; Dunn, E.; Carroll, S.; Bahena, E.M.; Patel, D.K.; Griffey, S.; Anvari, B. Biodistribution and Toxicological Evaluation of Micron- and Nano-Sized Erythrocyte-Derived Optical Particles in Healthy Swiss Webster Mice. Biomater. Sci. 2019, 7, 2123–2133.
47. Tang, J.C.; Vankayala, R.; Mac, J.T.; Anvari, B. RBC-Derived Optical Nanoparticles Remain Stable After a Freeze–Thaw Cycle. Langmuir 2020, 36, 10003–10011.
48. Liu, W.; Ruan, M.; Wang, Y.; Song, R.; Ji, X.; Xu, J.; Dai, J.; Xue, W. Light-Triggered Biomimetic Nanoerythrocyte for Tumor-Targeted Lung Metastatic Combination Therapy of Malignant Melanoma. Small 2018, 14, 1801754.
49. Gao, C.; Lin, Z.; Wang, D.; Wu, Z.; Xie, H.; He, Q. Red Blood Cell-Mimicking Micromotor for Active Photodynamic Cancer Therapy. ACS Appl. Mater. Interfaces 2019, 11, 23392–23400.
50. Flower, R.; Peiretti, E.; Magnani, M.; Rossi, L.; Serafini, S.; Gryczynski, Z.; Gryczynski, I. Observation of Erythrocyte Dynamics in the Retinal Capillaries and Choriocapillaris Using ICG-Loaded Erythrocyte Ghost Cells. Invest. Ophthalmol. Vis. Sci. 2008, 49, 5510–5516.
51. Ritter, S.C.; Milanick, M.A.; Meissner, K.E. Encapsulation of FITC to Monitor Extracellular PH: A Step towards the Development of Red Blood Cells as Circulating Blood Analyte Biosensors. Biomed. Opt. Express 2011, 2, 2012–2021.
52. Gao, M.; Hu, A.; Sun, X.; Wang, C.; Dong, Z.; Feng, L.; Liu, Z. Photosensitizer Decorated Red Blood Cells as an Ultrasensitive Light-Responsive Drug Delivery System. ACS Appl. Mater. Interfaces 2017, 9, 5855–5863.
53. Jiang, A.; Song, B.; Ji, X.; Peng, F.; Wang, H.; Su, Y.; He, Y. Doxorubicin-Loaded Silicon Nanoparticles Impregnated into Red Blood Cells Featuring Bright Fluorescence, Strong Photostability, and Lengthened Blood Residency. Nano Res. 2018, 11, 2285–2294.
54. Chen, Z.-A.; Wu, S.-H.; Chen, P.; Chen, Y.-P.; Mou, C.-Y. Critical Features for Mesoporous Silica Nanoparticles Encapsulated into Erythrocytes. ACS Appl. Mater. Interfaces 2019, 11, 4790–4798.
55. Gutiérrez Millán, C.; Castañeda, A.Z.; Sayalero Marinero, M.L.; Lanao, J.M. Factors Associated with the Performance of Carrier Erythrocytes Obtained by Hypotonic Dialysis. Blood Cells. Mol. Dis. 2004, 33, 132–140.
56. Bustamante López, S.C.; Meissner, K.E. Characterization of Carrier Erythrocytes for Biosensing Applications. J. Biomed. Opt. 2017, 22, 091510.

57. Marvin, C.M.; Ding, S.; White, R.E.; Orlova, N.; Wang, Q.; Zywot, E.M.; Vickerman, B.M.; Harr, L.; Tarrant, T.K.; Dayton, P.A.; et al. On Command Drug Delivery via Cell-Conveyed Phototherapeutics. Small 2019, 15, 1901442.
58. An, X.; Schulz, V.P.; Mohandas, N.; Gallagher, P.G. Human and Murine Erythropoiesis. Curr. Opin. Hematol. 2015, 22, 206–211.
59. Gordesky, S.E.; Marinetti, G.V. The Asymmetric Arrangement of Phospholipids in the Human Erythrocyte Membrane. Biochem. Biophys. Res. Commun. 1973, 50, 1027–1031.
60. Lang, F.; Lang, K.S.; Lang, P.A.; Huber, S.M.; Wieder, T. Mechanisms and Significance of Eryptosis. Antioxid. Redox Signal. 2006, 8, 1183–1192.
61. Wang, C.; Sun, X.; Cheng, L.; Yin, S.; Yang, G.; Li, Y.; Liu, Z. Multifunctional Theranostic Red Blood Cells For Magnetic-Field-Enhanced in Vivo Combination Therapy of Cancer. Adv. Mater. 2014, 26, 4794–4802.
62. Sun, X.; Wang, C.; Gao, M.; Hu, A.; Liu, Z. Remotely Controlled Red Blood Cell Carriers for Cancer Targeting and Near-Infrared Light-Triggered Drug Release in Combined Photothermal–Chemotherapy. Adv. Funct. Mater. 2015, 25, 2386–2394.
63. Jia, W.; Burns, J.M.; Villantay, B.; Tang, J.C.; Vankayala, R.; Lertsakdadet, B.; Choi, B.; Nelson, J.S.; Anvari, B. Intravital Vascular Phototheranostics and Real-Time Circulation Dynamics of Micro- and Nanosized Erythrocyte-Derived Carriers. ACS Appl. Mater. Interfaces 2020, 12, 275–287.
64. Weaver, J.C.; Chizmadzhev, Y.A. Theory of Electroporation: A Review. Bioelectrochem. Bioenerg. 1996, 41, 135–160.
65. Mac, J.T.; Vankayala, R.; Patel, D.K.; Wueste, S.; Anvari, B. Erythrocyte-Derived Optical Nanoprobes Doped with Indocyanine Green-Bound Albumin: Material Characteristics and Evaluation for Cancer Cell Imaging. ACS Biomater. Sci. Eng. 2018, 4, 3055–3062.
66. Mojzisova, H.; Bonneau, S.; Vever-Bizet, C.; Brault, D. Cellular Uptake and Subcellular Distribution of Chlorin E6 as Functions of PH and Interactions with Membranes and Lipoproteins. Biochim. Biophys. Acta BBA-Biomembr. 2007, 1768, 2748–2756.
67. Sun, L.; Li, Q.; Hou, M.; Gao, Y.; Yang, R.; Zhang, L.; Xu, Z.; Kang, Y.; Xue, P. Light-Activatable Chlorin E6 (Ce6)-Imbedded Erythrocyte Membrane Vesicles Camouflaged Prussian Blue Nanoparticles for Synergistic Photothermal and Photodynamic Therapies of Cancer. Biomater. Sci. 2018, 6, 2881–2895.
68. Kalchenko, V.; Shivtiel, S.; Malina, V.; Lapid, K.; Haramati, S.; Lapidot, T.; Brill, A.G.; Harmelin, A. Use of Lipophilic Near-Infrared Dye in Whole-Body Optical Imaging of Hematopoietic Cell Homing. J. Biomed. Opt. 2006, 11, 050507.

69. Flower, R.W.; Kling, R. Observation and Characterization of Microvascular Vasomotion Using Erythrocyte Mediated ICG Angiography (EM-ICG-A). Microvasc. Res. 2017, 113, 78–87.
70. Fang, R.H.; Hu, C.-M.J.; Chen, K.N.H.; Luk, B.T.; Carpenter, C.W.; Gao, W.; Li, S.; Zhang, D.-E.; Lu, W.; Zhang, L. Lipid-Insertion Enables Targeting Functionalization of Erythrocyte Membrane-Cloaked Nanoparticles. Nanoscale 2013, 5, 8884.
71. Wang, P.; Li, X.; Yao, C.; Wang, W.; Zhao, M.; El-Toni, A.M.; Zhang, F. Orthogonal Near-Infrared Upconversion Co-Regulated Site-Specific O2 Delivery and Photodynamic Therapy for Hypoxia Tumor by Using Red Blood Cell Microcarriers. Biomaterials 2017, 125, 90–100.
72. Wang, P.; Wang, X.; Luo, Q.; Li, Y.; Lin, X.; Fan, L.; Zhang, Y.; Liu, J.; Liu, X. Fabrication of Red Blood Cell-Based Multimodal Theranostic Probes for Second Near-Infrared Window Fluorescence Imaging-Guided Tumor Surgery and Photodynamic Therapy. Theranostics 2019, 9, 369–380.
73. Diamandis, E.P.; Christopoulos, T.K. The Biotin-(Strept)Avidin System: Principles and Applications in Biotechnology. Clin. Chem. 1991, 37, 625–636.
74. Tang, W.; Zhen, Z.; Wang, M.; Wang, H.; Chuang, Y.-J.; Zhang, W.; Wang, G.D.; Todd, T.; Cowger, T.; Chen, H.; et al. Red Blood Cell-Facilitated Photodynamic Therapy for Cancer Treatment. Adv. Funct. Mater. 2016, 26, 1757–1768.